Isotropic third-order statistics in turbulence with helicity: the 2/15-law

By SUSAN KURIEN[1], MARK A. TAYLOR[2]† AND TAKESHI MATSUMOTO[3]

[1] Center for Nonlinear Studies and Theoretical Division, Los Alamos National Laboratory, Los Alamos, NM 87545, USA

[2] Computer and Computational Sciences Division, Los Alamos National Laboratory, Los Alamos, NM 87545, USA

[3] Department of Physics, Kyoto University, Kitashirakawa Oiwakecho Sakyo-ku, Kyoto 606-8502, Japan

(Received 2 April 2004)

The so-called 2/15-law for two-point, third-order velocity statistics in isotropic turbulence with helicity is computed for the first time from a direct numerical simulation of the Navier-Stokes equations in a 512^3 periodic domain. This law is a statement of helicity conservation in the inertial range, analogous to the benchmark Kolmogorov 4/5-law for energy conservation in high-Reynolds number turbulence. The appropriately normalized parity-breaking statistics, when measured in an arbitrary direction in the flow, disagree with the theoretical value of 2/15 predicted for isotropic turbulence. They are highly anisotropic and variable and remain so over a long times. We employ a recently developed technique to average over many directions and so recover the statistically isotropic component of the flow. The angle-averaged statistics achieve the 2/15 factor to within about 7% instantaneously and about 5% on average over time. The inertial- and viscous-range behavior of the helicity-dependent statistics and consequently the helicity flux, which appear in in the 2/15-law, are shown to be more anisotropic and intermittent than the corresponding energy-dependent reflection-symmetric structure functions, and the energy flux, which appear in the 4/5-law. This suggests that the Kolmogorov assumption of local isotropy at high Reynolds numbers needs to be modified for the helicity-dependent statistics investigated here.

1. Introduction

There are two invariants of the inviscid Navier-Stokes equations – the total energy, defined by $E = \frac{1}{2}\int \mathbf{u}(\mathbf{x})^2 d\mathbf{x}$, and the total helicity $H = \int \mathbf{u}(\mathbf{x}) \cdot \boldsymbol{\omega}(\mathbf{x}) d\mathbf{x}$ where the vorticity $\boldsymbol{\omega}(\mathbf{x}) = \nabla \times \mathbf{u}(\mathbf{x})$. Energy has been extensively studied especially in statistical theories of turbulence as well as in experiments. Helicity, being sign-indefinite has been more challenging to study theoretically. Direct experimental measurements of helicity are also difficult because of the need to measure local gradients, requiring high resolution and careful probe design (see for example Kholmyansky *et al.* (2001)). Nevertheless, since the discovery of helicity as a conserved quantity by Moreau (1961) and independently by Moffat (1969), there have been several attempts to draw parallels with the energy

† Present address: Evolutionary Computing, Sandia National Laboratory, Albuquerque 87185, USA

dynamics. The existence of a helicity cascade was proposed by Brissaud *et al.* (1973) and various possible inertial range scalings of the energy and helicity spectra were discussed. The joint forward (downscale) cascade of energy and helicity has been verified in direct numerical simulations, most recently by Chen *et al.* (2003*a*). It was believed for some time that helicity, though an invariant, played an essentially passive role in turbulence. A recent work by three of us, Kurien *et al.* (2004), showed that there is a relevant timescale for helicity transfer in wavenumber space. The proper consideration of the helicity flux timescale showed that helicity can modify the energy dynamics, measureably slowing it down in the high wavenumbers.

We present a study of the small-scale phenomenology of turbulence with helicity in the manner of the Kolmogorov (1941) investigation (K41) of helicity-free turbulence. Using the Kármán-Howarth equation for the dynamics of the second-order two-point correlation function (see von Kármán & Howarth (1938)), Kolmogorov (1941) derived the benchmark 4/5 energy law for isotropic, reflection-symmetric (helicity-free), homogeneous turbulence, assuming finite mean energy dissipation ε as $\nu \to 0$,

$$\langle (u_L(\mathbf{x}+\mathbf{r}) - u_L(\mathbf{x}))^3 \rangle = -\frac{4}{5}\varepsilon r \tag{1.1}$$

for $\eta \ll r \ll L_0$, the so-called inertial range. η is the Kolmogorov dissipation scale and L_0 is the typical large scale. $u_L(\mathbf{x}) = \mathbf{u}_L(\mathbf{x}) \cdot \hat{\mathbf{r}}$ is the longitudinal component of $\mathbf{u}$ along $\hat{\mathbf{r}}$. $\langle \cdot \rangle$ denotes a suitable average. Kolmogorov required this to be an ensemble average of a high-Reynolds number, unforced (slowly decaying) flow. It has been shown empirically and proved that this is equivalent to a long-time average in statistically steady turbulence Frisch (1995). In statistically steady state at sufficiently high Reynolds number, the mean energy flux in the inertial range equals the mean dissipation rate $\varepsilon = 2\nu\langle |\nabla \mathbf{u}|^2 \rangle$ which is obtained by ensemble-averaging or time-averaging over the entire flow domain. The 4/5-law is a statement of the conservation of energy in the inertial range scales – the third-order structure function is an indirect measure of the flux of energy through scales of size r. A key assumption of the K41 theory was 'local isotropy' or isotropy of the small scales $r \ll L_0$ at sufficiently high Reynolds number. With this assumption, Eq. (1.1) should be recovered independent of the direction of $\hat{\mathbf{r}}$. This is why high Reynolds number experimental measurements of the K41 4/5-law have been successful even when the data are acquired in only a single direction in the flow (Sreenivasan & Dhruva (1998)).

Recently, a local version of the K41 statistical laws were proved in Duchon & Robert (2000); Eyink (2003): Given *any* local region B of size R of the flow, for $r \ll R$, and in the limits $\nu \to 0$, next $r \to 0$, and finally $\delta \to 0$,

$$\begin{aligned} \langle (\Delta u_L)^3 \rangle_{(\Omega,B)} &= \lim_{\delta \to 0} \frac{1}{\delta} \int_t^{t+\delta} d\tau \int \frac{d\Omega}{4\pi} \int_B \frac{d\mathbf{x}}{R^3} [\Delta u_L(\mathbf{r};\mathbf{x},\tau)]^3 \\ &= -\frac{4}{5}\varepsilon_B r. \end{aligned} \tag{1.2}$$

for almost every (Lebesgue) point t in time, where $\Delta u_L(\mathbf{r}) = u_L(\mathbf{x}+\mathbf{r}) - u_L(\mathbf{x})$ and ε_B is the instantaneous mean energy dissipation rate over the local region B. The angle integration $d\Omega$ integrates in $\mathbf{r}$ over the sphere of radius r. For each point $\mathbf{x}$ the vector increment $\mathbf{r}$ is allowed to vary over all angles and the resulting longitudinal moments are integrated. The integration over $\mathbf{x}$ is over the flow subdomain B. This version of the K41 result does not require isotropy, homogeneity of stationarity of the flow. Long-time or ensemble averages are also not required as in the original K41 theory. Eq. (1.2) is a version of K41 which is truly local in space and time. This version of the 4/5-law has not yet been rigorously verified empirically. It was shown by Taylor *et al.* (2003) that averaging the

third-order structure function over a large (finite) number of directions, that is, allowing $\hat{\mathbf{r}}$ to vary over angles for a fixed separation length r, gave results consistent with the 4/5-law at any given instant of the flow. At the very least, the 4/5-law does not seem to require isotropy, or long-time or ensemble averaging to hold; at any instant of a sufficiently 'high' Reynolds number flow, averaging over many angles, and over the whole domain appear to be sufficient.

The first attempt to study the symmetry and dynamics of the two-point correlation function in flows with helicity was made by Betchov (1961). Analogous to the K41 4/5-law, the so-called 2/15-law for homogeneous, isotropic turbulence with helicity was derived by different means by Chkhetiani (1996); L'vov *et al.* (1997); Kurien (2003),

$$\langle \Delta u_L(\mathbf{r})(u_T(\mathbf{x}+\mathbf{r}) \times u_T(\mathbf{x}))\rangle = \frac{2}{15} h r^2 \tag{1.3}$$

where the transverse component of the velocity $u_T(\mathbf{x}) = \mathbf{u}(\mathbf{x}) - u_L(\mathbf{x})$; the mean helicity flux which equals the mean helicity dissipation rate in steady state is $h = 2\nu\langle(\partial_j u_i)(\partial_j \omega_i)\rangle$, where the vorticity $\boldsymbol{\omega} = \nabla \times \mathbf{u}$. Once again $\langle\cdot\rangle$ denotes an ensemble average or average over long times in steady-state turbulence. We shall use the notation

$$H_{LTT}(\mathbf{r}) = \langle \Delta u_L(\mathbf{x})(u_T(\mathbf{x}+\mathbf{r}) \times u_T(\mathbf{x}))\rangle \tag{1.4}$$

to denote the third-order helical statistics. The quantity $H_{LTT}(\mathbf{r})$ is the simplest third-order velocity correlation which can have a spatially isotropic component while at the same time displaying a 'handedness' due to the cross-product in its definition (Eq. (1.3)). $H_{LTT}(\mathbf{r})/r^2$ is a measure of the helicity flux through scales of size r in the inertial range which must balance the helicity dissipation h in the viscous range for statistically steady turbulence. The derivation of the 2/15-law assumes inertial-range behavior of helicity in some range of scales $\eta \ll r \ll L_0$. A local version, as in Eq. (1.2), of the 2/15-law has not been derived. A shell model calculation by Biferale *et al.* (1998) has demonstrated the likelihood of the 2/15-law. However it has never been measured in experiments or, until the present work, in direct numerical simulations of the Navier-Stokes equations.

In this paper we present the first direct numerical simulations measurement of the 2/15-law for helicity conservation in the inertial range. In the next section we will describe the simulations and the calculation of the statistical quantities of interest for the 2/15-law. We will present a comparison with the 4/5-law calculation of the same flow, highlighting the differences between energy and helicity dynamics. We show that in the inertial range the helicity flux is more anisotropic and intermittent than the energy flux; and that the smallest resolved scales show recovery of isotropy for energy-dependent statistics but show persistent anisotropy for helicity-dependent statistics over the 10 large-eddy turnover times for which simulation ran. We will conclude with some final remarks on what our analysis means for future work in the area of helicity dynamics and parity-breaking in turbulent flows.

2. Simulations and Results

We performed a simulation of the forced Navier-Stokes equation in a unit-periodic box with 512 grid points to a side. In these units the wavenumber k is in integer multiples of 2π. The forcing scheme was the deterministic forcing of Taylor *et al.* (2003), modeled after the deterministic forcing used in Chen *et al.* (2003*a*). This forcing simply relaxes the Fourier coefficients in the first two wave numbers so that the energy matches a prescibed target spectrum $F(k) = 0.5$ $(k = 1, 2)$. The forcing does not change the phases of the coefficients, which are observed to change slowly in time. In addition, maximum helicity

N	ν	R_λ	E	ε	H	h	$k_{\max}\eta$
512	10^{-4}	270	1.72	1.51	-26.8	62.2	1.1

TABLE 1. Parameters of the numerical simulation. ν - viscosity; R_λ - Taylor Reynolds number; mean total energy $E = \frac{1}{2}\sum_k \tilde{\mathbf{u}}(\mathbf{k})^2$; ε - mean energy dissipation rate; mean total helicity $H = \sum_k \tilde{\mathbf{u}}(\mathbf{k}) \cdot \tilde{\boldsymbol{\omega}}(\mathbf{k})$; h - mean helicity dissipation rate; Kolmogorov dissipation scale $\eta = (\nu^3/\varepsilon)^{3/4}$.

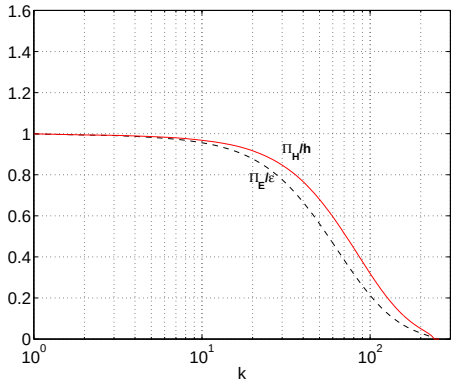

FIGURE 1. Dotted line: Flux of energy Π_E normalized by mean dissipation rate of energy ε. Solid line: Flux of helicity Π_H normalized by mean dissipation rate of helicity h.

was injected into the wavenumbers 1 and 2 using the scheme of Polifke & Shtilman (1989). The calculation ran for 10 large-eddy turnover times. The flow achieved steady state in about 1 large-eddy turnover time. The statistics reported here have been calculated over a total of 45 frames spanning the latter 9 eddy turnover times. The same data were reported in Kurien *et al.* (2004). Some additional parameters of the simulation are given in Table 1. Figure 1 shows the mean energy and helicity fluxes normalized by the mean energy and helicity dissipation rates respectively. Note the close to decade range of wavenumbers where ε and h match the energy and helicity fluxes respectively very well.

2.1. *Third-order helical velocity statistics and the use of angle-averaging*

We first define the compensated quantity

$$\widetilde{H}_{LTT}(\mathbf{r}) = H_{LTT}(\mathbf{r})/(h\ r^2). \tag{2.1}$$

In Fig. 2(a) we show $\widetilde{H}_{LTT}(\mathbf{r})$ calculated from a single frame arbitrarily chosen after the flow achieved statistically steady state. Each dotted line is $\widetilde{H}_{LTT}(\mathbf{r})$ in one of 73 different directions in the flow, as a function of scale size r. The directions are fairly uniformly distributed over the sphere (see Taylor *et al.* (2003) for how these directions were chosen). None of the curves show a tendency towards the theoretically predicted $2/15 = 0.1\dot{3}$ value for an extended range of scales. Among the calculations shown are those for the three coordinate directions which are the most often reported in statistical turbulence studies. For any given r the different directions yield vastly different values. Exceptional are the very largest (forced) scales where the different directions appear to converge. This is already signals something different than the usual expectation that anisotropy, if any, should come from, and dominate in, the large scales. Overall angular dependence (anisotropy) plays a strong role in these statistics. In this snapshot of the

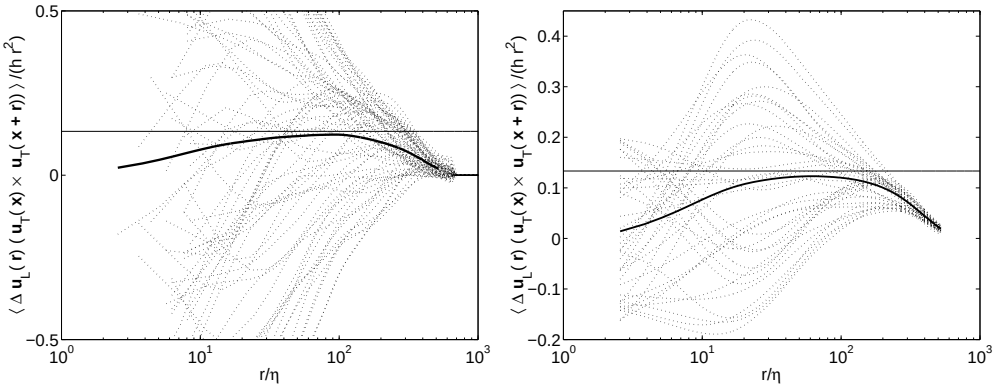

(a) $\widetilde{H}_{LTT}(\mathbf{r})$ in 73 different directions of the flow (dotted lines) from a single frame after the flow has reached statistically steady state. The thick solid line is the mean over all the directions.

(b) The time-average of $\widetilde{H}_{LTT}(\mathbf{r})$ in each of the 73 different directions (dotted lines) and of the angle-average (thick solid line).

FIGURE 2. Instantaneous and time-averaged 2/15 law calculations. The 2/15 value is indicated by the horizontal line in both plots. The inertial range is gauged from those length scales where the angle-averaged curve most closely approaches 2/15 and is roughly estimated to be $30 < r < 150$. Note that the vertical scale in the two plots is not the same; the time-averaged quantities on the right have significantly reduced spread compared to the instantaneous quantities on the left.

flow the anisotropy persists strongly into the smallest resolved scales, as seen in the large spread of values among the different directions at $r/\eta \approx 2$, where we might expect viscous effects are important. Indeed it appears that it would be fortuitous for an arbitrary direction of the flow to yield the correct theoretical prediction for isotropic flow.

Next we extract the isotropic component of these statistics by employing the angle-averaging technique used in Taylor *et al.* (2003). In effect, we average the statistics for a given r over all the directions to get the angle-averaged mean isotropic (angle-independent) contribution. This is the thick solid curve in Fig. 2(a). It approaches the 2/15 line rather closely in the range $30 < r/\eta < 150$. The peak value of the thick curve is ≈ 0.124 which is within about 7% of the 2/15 value. This is a remarkable result out of a single snapshot; there is no *a priori* reason to expect that angle-averaging an arbitrarily chosen, highly anisotropic snapshot, will yield consistency with the 2/15-law which was derived for isotropic flow. We believe that this result is strong motivation for the existence of a local 2/15 law analogous to the local 4/5-law of Eyink (2003). Despite the lack of a proof we will write down the corresponding local 2/15-law based on our empirical results,

$$\begin{aligned}\langle \Delta u_L(\mathbf{r})(u_T(\mathbf{x}+\mathbf{r})\times u_T(\mathbf{x}))\rangle_{(\Omega,B)} &= \lim_{\delta\to 0}\frac{1}{\delta}\int_t^{t+\delta} d\tau \int \frac{d\Omega}{4\pi}\int_B \frac{d\mathbf{x}}{R^3} \\ &\quad\times [\Delta u_L(\mathbf{r};\mathbf{x},\tau)][(u_T(\mathbf{x}+\mathbf{r})\times u_T(\mathbf{x}))] \\ &= \frac{2}{15}h_B r^2. \end{aligned} \tag{2.2}$$

where Ω, B, R and t have the same meanings as for Eq. (1.2); h_B denotes the locally (in space and time) averaged helicity dissipation rate. We emphasize that there is as yet no proof for Eq. (2.2); we have merely written down a conjecture by analogy to Eq. (1.2) and

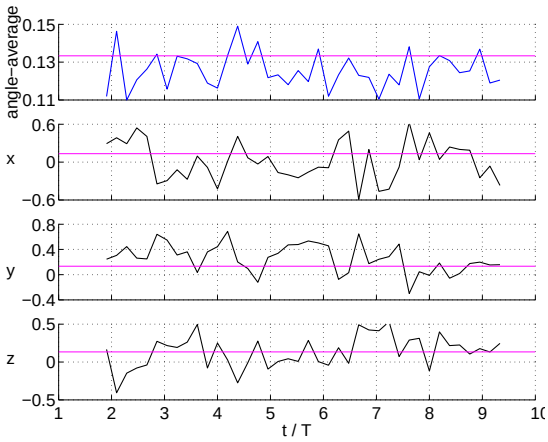

FIGURE 3. The value of $\widetilde{H}_{LTT}(\mathbf{r})$ in the middle of the inertial range ($r/\eta \approx 65$) as a function of number of eddy turnover times. From top to bottom: Angle-averaged, x-direction, y-direction, z-direction. Note that the vertical scales in the four panels are not the same; the bottom three panels corresponding to the coordinate directions have a much greater spread of values than the top panel for the angle-average. The mean and standard deviations for each case are given in Table 2.

Inertial range	2/15-law	4/5-law
Theory	$0.13\dot{3}$	0.8
Angle-avg	0.126 ± 0.009	0.75 ± 0.03
x	0.02 ± 0.31	0.78 ± 0.14
y	0.26 ± 0.23	0.75 ± 0.13
z	0.14 ± 0.21	0.76 ± 0.11

TABLE 2. Mean and standard deviation of the compensated third order statistics in the middle of the inertial range.

motivated by our calculation of the 2/15-law for a single snapshot of the fully developed flow.

In order to check if the anisotropy observed in a single frame persists over time, we averaged $\widetilde{H}_{LTT}(\mathbf{r})$ in each of the 73 different directions over 9 large-eddy turnover times (45 frames). We performed the same time-average for the angle-average. The result is shown in Fig. 2(b). The spread in the inertial-range decreased by about a factor of 2 while the spread in the smallest scales decreased by a factor of about 6 relative to the single-frame statistics of Fig. 2(a). Inspite of this, the residual variance is significant as we demonstrate in Fig. 3 and as compared below to the same analysis done for the 4/5-law. We plot a time-trace of the peak value of the angle-averaged $\widetilde{H}_{LTT}(r)$ in the top panel of Fig. 3. The angle-averaged value is 0.126 ± 0.009, within error of the predicted value of $2/15 = 0.1\dot{3}$. Since most prior numerical simulations investigations have studied two-point statistics in the coordinate directions only, we present in the bottom three panels of Fig. 3, the values of $\widetilde{H}_{LTT}(\mathbf{r})$ at $r/\eta = 65$ (i.e. more or less the middle of the inertial range on a logarithmic scale) for $\hat{\mathbf{r}}$ in the x-, y- and z-directions respectively as a function of time. Table 2 (column 2) shows the mean and standard deviation for each of the four time-trace plots of Fig. 3. The first thing to notice is that none of the coordinate directions average to 2/15 over long times. This behavior demonstrates that these statistics are highly anisotropic and remain so over long times. Secondly, the

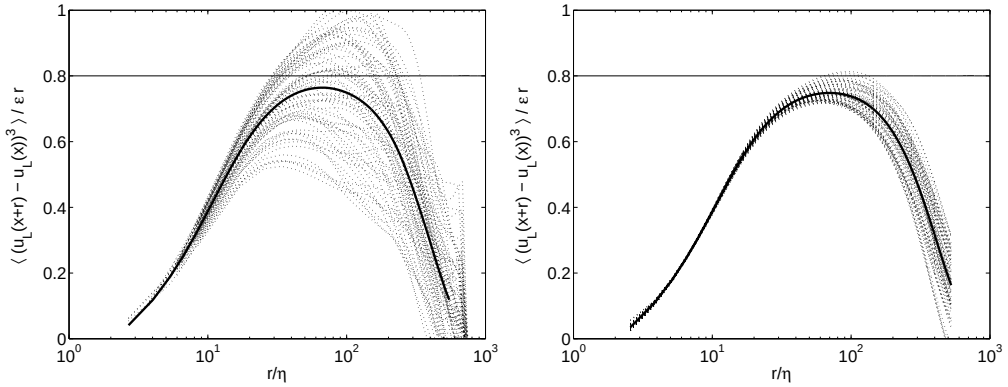

(a) $\widetilde{S}_{L,3}(\mathbf{r})$ in 73 different directions of the flow (dotted lines) from an arbitrarily chosen frame after the flow has achieved statistical equilibrium. The thick solid line is the mean over all the directions.

(b) The time-average of $\widetilde{S}_{L,3}(\mathbf{r})$ in each of the 73 different directions (dotted lines) and of the angle-average (thick solid line).

FIGURE 4. Instantaneous and time-averaged calculations of the 4/5-law. The 4/5 value is indicated by the horizontal line in both plots.

mean values in the coordinate directions are poorly defined and practically meaningless in the sense of having extremely large standard deviations; the measured values though often coming close to $0.1\dot{3}$, are highly variable for a particular direction. In turbulence phenomenology, such large jumps in values from their mean is the signature of intermittency; the presence of strong, anomalous events. We conclude that the helicity flux in a particular direction is highly intermittent in the inertial range. This supports the conclusion of Chen *et al.* (2003*b*), who showed that helicity flux was more intermittent than energy flux by measuring the scaling exponents of flux-related quantities.

2.2. *Comparative analysis of the 4/5-law*

We compare these results with the analogous ones for the 4/5-law for the same flow. As before, we define the compensated third-order longitudinal structure function

$$\widetilde{S}_{L,3}(\mathbf{r}) = \langle (u_L(\mathbf{x}+\mathbf{r}) - u_L(\mathbf{x}))^3 \rangle / (\varepsilon r). \tag{2.3}$$

Figure 4(a) shows a single frame calculation of $\widetilde{S}_{L,3}(\mathbf{r})$ for 73 different directions as a function of r (dotted lines). We performed the angle-averaging exactly as in Taylor *et al.* (2003) to recover the isotropic mean (thick solid line). Our first observation is that the 4/5-law is recovered in this helical flow to as good a degree as in the simulation with zero mean helicity of Taylor *et al.* (2003). This demonstrates that the reflection-symmetry assumption of Kolmogorov, under which the 4/5-law was derived, need not hold in order to see this result. This is understood by the fact that the lowest-order (unclosed) dynamical equations for the symmetric second-order correlation functions (von Kármán & Howarth (1938)) from which the 4/5-law was derived by Kolmogorov (1941), decouple from their antisymmetric counterpart (Betchov (1961)) from which the 2/15-law was derived by Kurien (2003). The third-order longitudinal structure functions of the K41 law are reflection-symmetric by definition, and therefore do not directly probe the helical, parity-breaking properties of the flow; correspondingly the third-order cor-

relation function H_{LTT} of the 2/15-law, measured here for the first time, do not probe the reflection-symmetric properties of the flow. The 4/5- and 2/15-laws in fact coexist in turbulent flows with helicity. This possibility was first hinted at by Betchov (1961), where he noted that in the hierarchy of moments, the fourth-order correlation function is the lowest order at which coupling of the symmetric (energy-dependent) and antisymmetric (helicity-dependent) quantities can occur.

There is a marked qualitative difference between the snapshot of Fig. 4(a) and the corresponding calculation of the 2/15-law in Fig. 2(a). The anisotropy (angular-dependence) is far smaller in a single snapshot of the 4/5-law as compared to the analogous 2/15-law calculation, both in the inertial range as well as in the viscous range. We will discuss the latter effect in section 2.3. In the inertial range, we see in Fig. 4(b), that the time-averaged compensated third-order longitudinal structure function for all the directions converge rather well relative to the single frame in Fig. 4(a). There is still significant spread of values among the different directions in the inertial range but it is far less than in the time-averaged 2/15-law calculation in Fig. 2(b). To make a more quantitative comparison, we present the mid-inertial-range values of the angle-averaged, and the x-, $y-$ and $z-$direction calculations in Table 2, column 3. The time mean for the angle-average is well-defined at 0.75 ± 0.03, a small standard deviation of 4%. The means in the coordinate directions range from 0.75 to 0.78, not intolerably far from the 0.8 value expected from theory, but with significant standard deviation in time of the order of 20%. Still, the behavior is very different from the 2/15-law statistics (Table 2, column 2), where not only was the 2/15 value not achieved in an arbitrary direction, but the variability in time was huge, 100% or more. We are lead to conclude that in the inertial range, both instantaneously and over long times, the helicity flux (as described by the 2/15-law) is far more anisotropic and intermittent than the energy flux (as described by the 4/5-law) for the same statistically steady flow.

2.3. *The viscous range*

As already noted, anisotropy of $\widetilde{H}_{LTT}$ persists into the smallest resolved scales as demonstrated by the large variance among the directions in the range $r/\eta < 10$ in Figs. 2(a) and 2(b). By contrast, the angular-dependence of $\widetilde{S}_{L,3}(\mathbf{r})$ becomes very small in the same range in a snapshot (Fig. 4(a)) and even more so on average over time (Fig. 4(b)). In these scales the 2/15- and 4/5-laws no longer hold as viscous effects become important; the quantities $\widetilde{H}_{LTT}$ and $\widetilde{S}_{L,3}$ no longer correspond strictly to the helicity and energy fluxes respectively. The viscous terms for the symmetric quantities, interpreted as energy dissipation at scales $r \approx \eta$, are strictly a sink for energy, pulling energy out of the flow. As is well known, the viscous terms for the antisymmetric quantities, correspondingly the helicity-dissipation at scales $r \approx \eta$, may be positive (producing helicity) or negative (removing helicity). Nevertheless, if the small scale statistics H_{LTT} are to be isotropic, the different directions might be expected to converge in the very small scales. In Table 3, column 2, we show time-mean and standard deviation of the angle-average and the x-, y- and z-direction calculations of $H_{LTT}(\mathbf{r})$ at $r/\eta \approx 2$. The time-mean angle-averaged value is about 0.014 ± 0.004, a standard deviation of about 30%. Again as in the inertial range, the time-average in a particular direction does not agree with the angle-averaged value and the standard deviations are enormous. We have shown the corresponding numbers for the 4/5-law for comparison (Table 3, column 3); the means in a particular direction agree better with the angle-averaged mean, and the variances are around 5%, indicating recovery of isotropy in the small-scales and relatively weaker intermittency than for the 2/15-law statistics. We here introduce a note of caution about the results in the viscous range as our simulation is only resolved upto $r/\eta \approx 2$ ($k_{\max}/\eta \approx 1.1$). While the

Viscous range	2/15-law	4/5-law
Angle-avg	0.014 ± 0.004	0.035 ± 0.006
x	-0.05 ± 0.65	0.057 ± 0.004
y	0.02 ± 0.57	0.055 ± 0.003
z	0.17 ± 0.55	0.057 ± 0.003

TABLE 3. Mean and standard deviation of the compensated third order statistics for the smallest resolved scale.

inertial range is amply resolved, the viscous range might display some residual effects of being under-resolved. Nevertheless, to the extent that in the *same* flow, the energy-dependent statistics seem to recover isotropy rather quickly in the viscous scales, it seems appropriate to point out that the helicity-dependent statistics remain dramatically and persistently anisotropic in the viscous scales over the long duration of our simulation.

3. Conclusions

There are three main points to be extracted from our first analysis of the 2/15-law. First, this analysis shows that a *local* version of the 2/15-law analogous to the local 4/5-law of Duchon & Robert (2000); Eyink (2003), might hold true; we hope our empirical results motivate a theoretical effort towards a proof. Second, the helicity flux is significantly more anisotropic and intermittent than the energy flux. The related third-order statistics H_{LTT} remain highly anisotropic all the way into the viscous scales. This suggests that the viscous generation and dissipation of helicity in the small scales is highly anisotropic as well. This might be related to the strong helical events seen in the transverse alignment of vortices in the work of Holm & Kerr (2002). Third, there is an underlying isotropic component of the flow which is extracted by the angle-averaging procedure of Taylor *et al.* (2003). It is not surprising that angle-averaging recovers the orientation-independent component of the field; this is merely the projection onto the one-dimensional (isotropic) component of the SO(3) group decomposition. However it is rather remarkable that this spherically averaged value tends to the predicted 4/5 and 2/15 values for $\widetilde{S}_{L,3}$ and $\widetilde{H}_{LTT}$ respectively. This results suggest that the 'local isotropy' requirement of K41 can be relaxed in favor of a hypothesis that the flow statistics have a universal underlying isotropic component which may be projected out.

We conclude with two remarks which were not explicitly mentioned in the body of this paper. The issues of anisotropy and intermittency of the small-scales of the flow are intimately connected with the particular kind of statistics measured. We have shown that in the same flow, certain statistics which depend on energy flux recover isotropy in the small scales, while others which depend on helicity do not. In this context it is more sensible to speak of isotropy (or lack of isotropy) of the *statistics* of the flow rather than of the $flow$ itself.

A second relevant remark is that our numerical data and analysis give some indication as to what might be expected when measuring $H_{LTT}(\mathbf{r})$ in high-Reynolds number experimental flows. In many such experiments, data is acquired at a few points over long times, and the statistics are obtained by applying Taylor's hypothesis to obtain the spatial correlations in a single-direction (for example, the streamwise direction in a windtunnel). Assuming there is some helicity in the flow, it might not be possible to predict the behavior of $H_{LTT}(\mathbf{r})$ for a particular direction $\hat{\mathbf{r}}$ (see Kholmyansky *et al.* (2001)). In this respect, the full-field information and angle-averaging technique appear

to be *fundamental* to recovering the 2/15 isotropic prediction. An experimental effort such as the three-dimensional velocity field imaging of Tao *et al.* (2002) could provide the kind of information required to see this 2/15-law experimentally. This is very different from measurement of the 4/5-law for energy, where, given a large enough scaling range (Reynolds number high enough), the statistics in any direction are observed to recover isotropy in the small scales.

We are grateful for useful discussions with D.D. Holm and G.L. Eyink.

REFERENCES

Betchov, R. 1961 Semi-isotropic turbulence and helicoidal flows. *Phys. Fluids* **4**, 925.

Biferale, L., Pierotti, D. & Toschi, F. 1998 Helicity transfer in turbulent models. *Phys. Rev. E* **57**, R2515–18.

Brissaud, A., Frisch, U., Leorat, J., Lesieur, M. & Mazure, A. 1973 Helicity cascades in fully developed isotropic turbulence. *Phys. Fluids* **16**, 1366–1377.

Chen, Q., Chen, S. & Eyink, G. L. 2003*a* The joint cascade of energy and helicity in three-dimensional turbulence. *Phys. Fluids* **15**, 361–374.

Chen, Q., Chen, S., Eyink, G. L. & Holm, D. 2003*b* Intermittency in the joint cascade of energy and helicity. *Phys. Rev. Lett.* **90**, 214503.

Chkhetiani, O. G. 1996 On the third-moments in helical turbulence. *JETP Lett.* **63**, 768–772.

Duchon, J. & Robert 2000 Inertial energy dissipation for weak solutions of incompressible euler and navier-stokes equations. *Nonlinearity* **13**, 249–255.

Eyink, G. 2003 Local 4/5-law and energy dissipation anomaly in turbulence. *Nonlinearity* **16**, 137–145.

Frisch, U. 1995 *Turbulence: The Legacy of A.N. Kolmogorov*. Cambridge University.

Holm, D. & Kerr, R. 2002 Transient vortex events in the initial value problem for turbulence. *Phys. Rev. Lett.* **88**, 244501/1–4.

von Kármán, T. & Howarth, L. 1938 On the statistical theory of isotropic turbulence. *Proc. R. Soc. Lond. A* **66**, 192–215.

Kholmyansky, M., Shapiro-Orot, M. & Tsinober, A. 2001 Experimental observations of spontaneous breaking of reflection symmetry in turbulent flow. *Proc. R. Soc. Lond. A* **457**, 2699–2717.

Kolmogorov, A. N. 1941 Dissipation of energy in locally isotropic turbulence. *Dokl. Akad. Nauk SSSR* **32**, 16–18.

Kurien, S. 2003 The reflection-antisymmetric counterpart of the kármán-howarth dynamical equation. *Physica D* **175**, 167–176.

Kurien, S., Taylor, M. & Matsumoto, T. 2004 Cascade timescales for energy and helicity in homogeneous isotropic turbulence. *Submitted to Phys. Rev. E* .

L'vov, V. S., Podivilov, E. & Procaccia, I. 1997 Exact result for the 3rd order correlations of velocity in turbulence with helicity. *chao-dyn/9705016* .

Moffat, H. K. 1969 The degree of knottedness of tangled vortex lines. *J. Fluid Mech.* **35**, 117–129.

Moreau, J. J. 1961 Constantes d'un îlot tourbillonnaire en fluide parfait barotrope. *C. R. Acad. Sci. Paris* **252**, 2810.

Polifke, W. & Shtilman, L. 1989 The dynamics of helical decaying turbulence. *Phys. Fluids A* **1**, 2025–2033.

Sreenivasan, K. R. & Dhruva, B. 1998 Is there scaling in high-Reynolds-number turbulence? *Progr. Theoret. Phys. Suppl.* (130), 103–120.

Tao, B., Katz, J. & Meneveau, C. 2002 Statistical geometry of subgrid-scale stresses determined from holographic particle image velocimetry measurements. *J. Fluid Mech.* **457**, 35–78.

Taylor, M., Kurien, S. & Eyink, G. L. 2003 Recovering isotropic statistics in turbulence simulations - the 4/5 law. *Phys. Rev. E* **68**, 26310–18.